ESI

for

A FA1-targeting albumin marker enables the ratiometric detection of apixaban in urine

Weihua Deng [a], Immanuel David Charles [a,] *, Zhongyong Xu [a], Taoyuze Lv [b], Lei Wang [a], Xiongzhi Xiang [a,]* and Bin Liu [a,] *

[a] Guangdong Provincial Key Laboratory of New Energy Materials Service Safety, College of Materials Science and Engineering, Shenzhen University, Shenzhen 518060, China.

[b] School of Physics, The University of Sydney, NSW 2006, Australia.

*Corresponding authors:

Charles Immanuel David, imanndavid@szu.edu.cn;

Xiongzhi Xiang, xiyun_cn@szu.edu.cn

Bin Liu, bliu@szu.edu.cn

1. Materials and methods

1.1 Materials

All chemicals were purchased from Shanghai Bide Pharmatech Co.Ltd, Shanghai Aladdin BioChem Technology Co.Ltd, and Shenzhen Changtai Chemical Technology Co.Ltd used without further purification. All biological analytes including apixaban (AP), human serum albumin (HSA), Na^+, Ca^{2+}, K^+, Cl^-, NO_3^-, SO_4^{2-}, lipase, carbolic anhydrase, lysozyme, cysteine (Cys), glutathione (GSH), glutamic acid (Glu), arginine (Arg), proline (Pro), tryptophan (Trp), urea, urine acid (UA), creatinine (Cre), cortisol, glucose, lactose (Lac), glycoproteins, trypsin and proteinase were purchased from Sigma-Aldrich Co.Ltd used without further purification. Phosphate buffered saline (PBS, 100 mM, pH ~7.4) was purchased from J&K scientific. The urine samples were obtained from healthy individual.

1.2 Instruments

^1H NMR and ^{13}C NMR spectra were measured by a Bruker AVANCE III 500-MHz spectrometer, respectively. HRMS was measured on a Thermo Fisher Q Exactive spectrometer. MALDI-TOF-MS experiments were carried out in a BRUKER autoflex speed MALDI-TOF mass spectrometer equipped with a 1000 HZ nitrogen laser. UV–Vis absorption and fluorescence spectra were tested by a Thermo-Fisher Evolution 220 and Thermo-Fisher Lumina fluorometer, respectively.

1.3 Construction of DMC@HSA

DMC@HSA solution (10 μM) was prepared by mixing 2 μL of DMC (10 mM in DMSO) and 40 μL of HSA (0.5 mM in water) into 2 mL of PBS buffer (1 mM, pH ~7.4).

1.4 Urine sample

Urine samples were voluntarily provided by the first author in this work who signed informed consent forms prior to collection, in accordance with the ethical research guidelines of our

institution. All experiments involving the collected samples were conducted in compliance with relevant laws and institutional guidelines. The study strictly adhered to the general principles outlined in the Declaration of Helsinki. All solution samples for spectral tests were diluted from stock solutions to proposed concentrations and mixed in sample bottles on a vortexer (2500 rpm) for 1 min. Urine samples were stored at -20 °C and used within 48 h. 2 μL of the DMC stock solution was mixed with 0.2 mL urine sample and 1.8 mL PBS buffer spiked of HSA (10 μM). All urine samples were vigorously vortexed for 1 min before recording on fluorometer.

1.5 Molecular docking

The 3D geometry of ligands (DMC and AP) were minimized by a mm2 job in Chem3D. The ligand-free crystal structure of albumin (PDB ID: 4k2c) was taken from the Brookhaven Protein Data Bank (http://www.rcsb.org/pdb). Flexible ligand docking was performed by AutoDock 4.2 molecular docking program using the implemented empirical free energy function and the Lamarckian Genetic Algorithm. The Autogrid was used to calculate Grids. The grid spacing was 0.375 Å as default. 20 docking runs with 25,000,00 energy evaluations were performed. Binding energy of each complex was recorded directly from AutoDock. The output from AutoDock was rendered with PyMol. The 2D diagrams were produced by a ligplus software.

1.6 Limit of detection

The limit of detection (LOD) for AP was calculated by using 3σ/κ rule based on concentration AP titration experiments. Where σ is the standard deviation of blank measurement for ten times and κ is the slope of the fluorescent intensity plotted against the AP concentration.

1.7 Calculation of binding constant (K_b) and stoichiometry (n)

The binding parameters can be calculated using fluorescence data. The calculation of binding constant (K_b) and binding stoichiometry (n) can be conducted based on the previously reported equations.[1]

$$\log\left(\frac{F_0 - F}{F}\right) = \log Kb + n \log [Q]$$

1.8 MALDI-TOF-MS

Matrix-Assisted Laser Desorption/Ionization Time-of-Flight (MALDI-TOF) mass characterization was conducted on a Bruker UltrafleXtreme TOF/TOF mass spectrometer (Bruker Daltonics, Inc, Billerica, MA) equipped with a Nd: YAG laser (355 nm). α-Cyano-4-hydroxycinnamic acid (CHCA, TCI, > 99%) was applied as the matrix. The matrix (conc. 20 mg/mL) was dissolved in H_2O/CH_3CN (1/1, v/v) at. Each sample was prepared by depositing 0.5 μL of matrix solution on the wells of a 384-well ground-steel plate, allowing the spots to dry, depositing 0.5 μL of the samples (HSA and DMC@HSA) on a spot of dry matrix, and adding another 0.5 μL of matrix on top of the dry sample. The plate was inserted into the MALDI source after drying. The mass scale was calibrated externally using polymethyl methacrylate at the molecular weight range under consideration in reflectron mode. Then, samples were tested in linear positive mode and the data analysis was conducted with Bruker's FlexAnalysis software.

1.9 Fluorescence lifetime

Fluorescent decay curves were recorded by a Horiba Delta-Flex instrument with a nanoLED with peak wavelength at 453 nm (pulse duration < 1.4 ns). Lifetime was recorded at peak wavelength. IRF is the instrument response function (prompt). The radiation decay curves were typically fit to the multi-exponential model: $I(t) = A + I_0 \cdot \sum \alpha_i \exp(-t/\tau_i)$. The I_0 represents the original fluorescent intensity; the α_i are pre-exponential factors, which represent the fractional amount of each lifetime component and the $\sum \alpha_i$ isormalized to unity; the τ_i refer to fluorescence lifetimes. The average fluorescence lifetime is calculated by equation: $\tau = \sum \alpha_i \tau_i$.

2. Figures and Tables

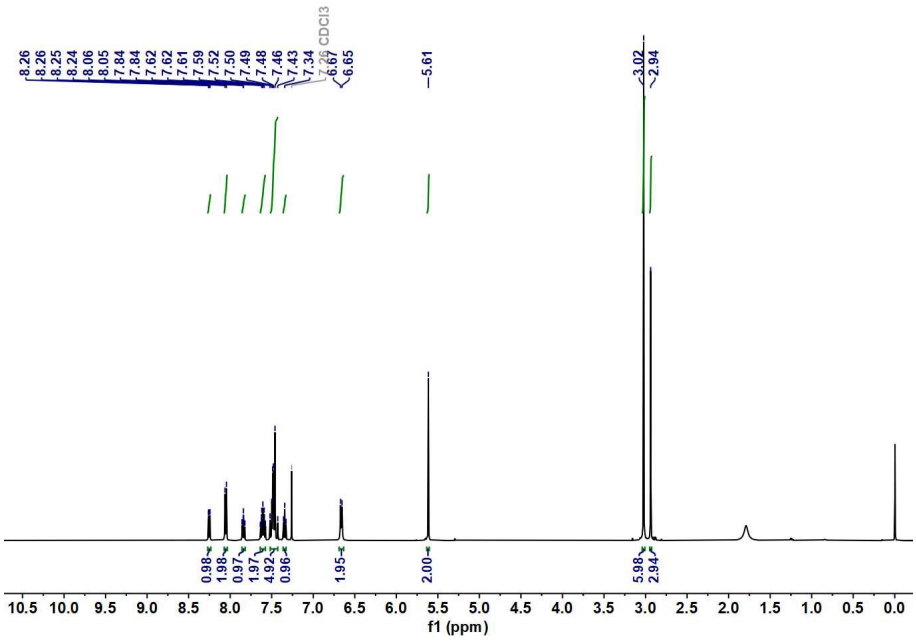

Fig. S1 ^{1}H NMR spectrum of DMC in $CDCl_3$

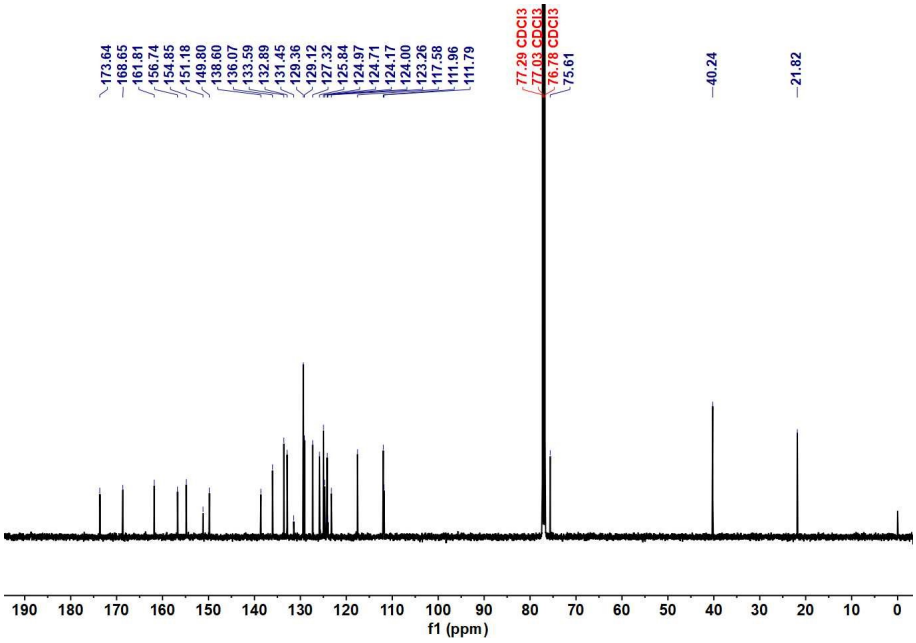

Fig. S2 ^{13}C NMR spectrum of DMC in $CDCl_3$

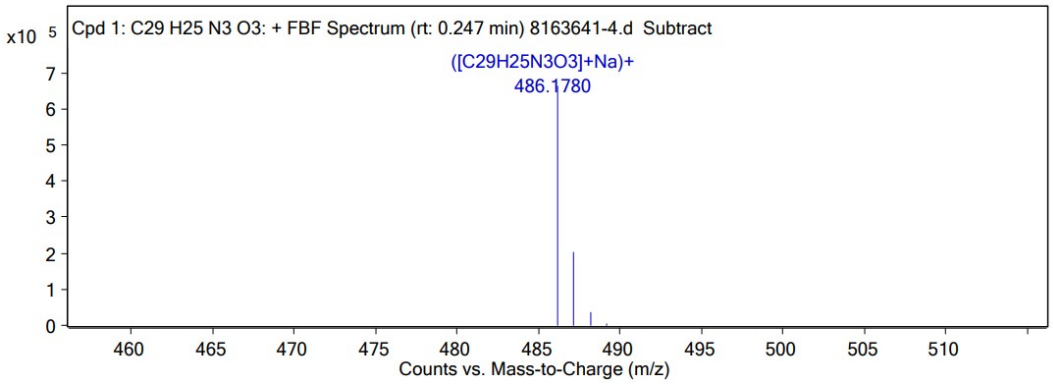

Fig. S3 HRMS spectrum of DMC

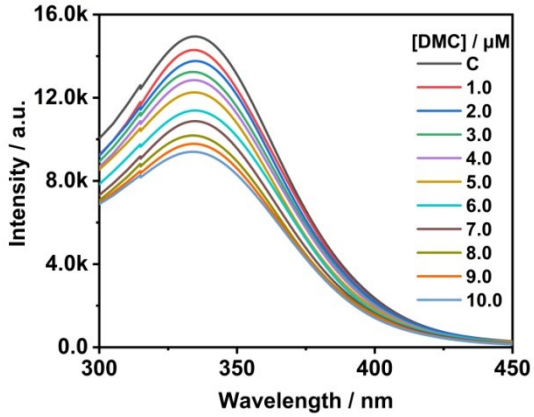

Fig. S4 The fluorescent spectra of HSA (10 μM) in the presence of DMC (0-10 μM). λ_{ex} = 280 nm.

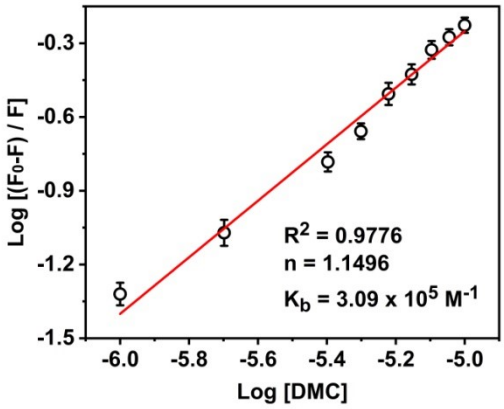

Fig. S5 The dependence of fluorescent signal [(F_0-F/F)] on concentrations of DMC. Error bars = ± SD, n = 3. λ_{ex} = 280 nm.

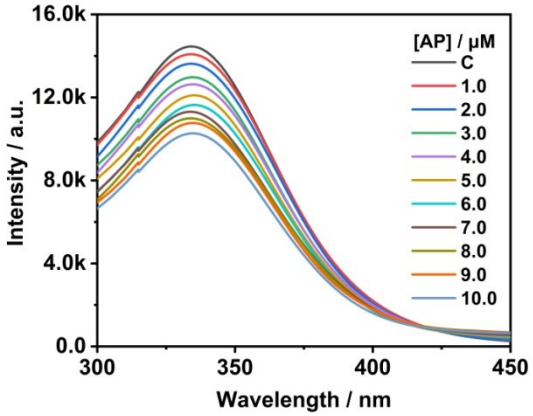

Fig. S6 The fluorescent spectra of HSA (10 μM) in the presence of AP (0-10 μM). λ_{ex} = 280 nm.

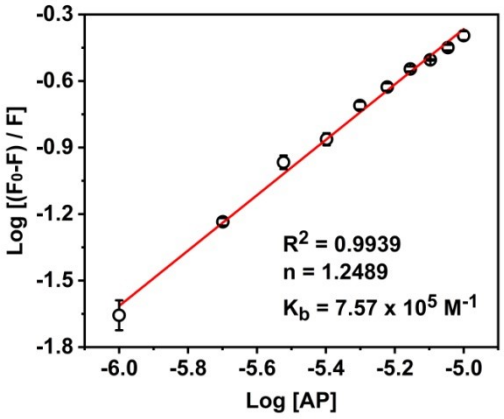

Fig. S7 The dependence of fluorescent signal [(F_0-F/F)] on concentrations of AP. Error bars = ± SD, n = 3. λ_{ex} = 280 nm.

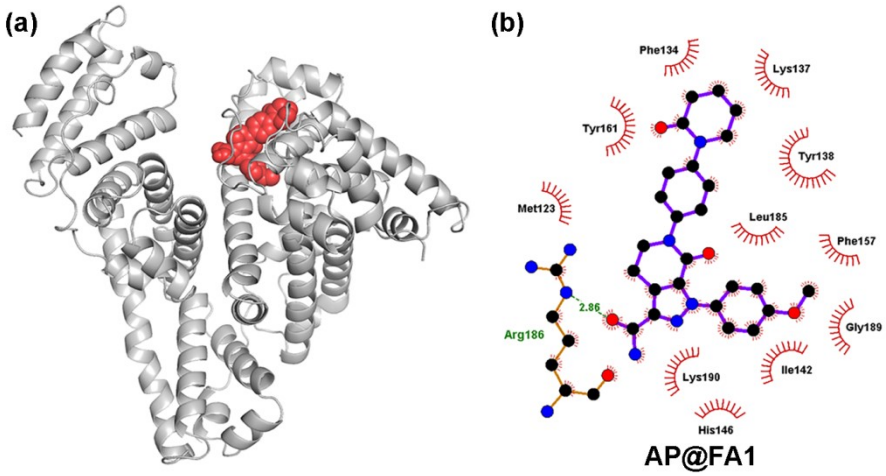

Fig. S8 Calculated binding mode of AP in FA1 sites of HSA. (a) 3D and (b) 2D diagrams are outputted by AutoDock and Ligplot, respectively.

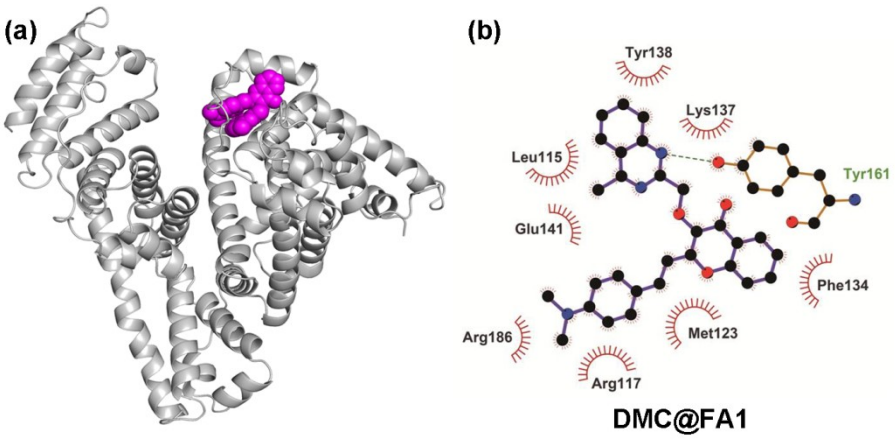

Fig. S9 Calculated binding mode of DMC in FA1 sites of HSA. (a) 3D and (b) 2D diagrams are outputted by AutoDock and Ligplot, respectively.

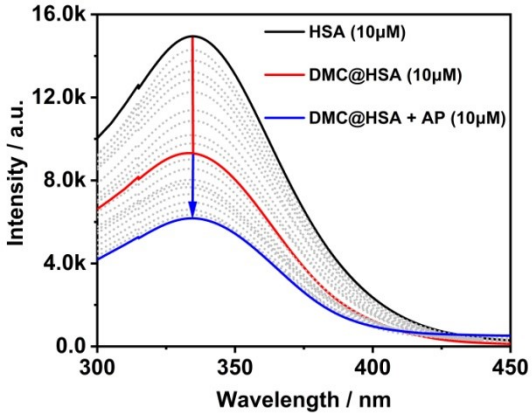

Fig. S10 The fluorescent spectra of HSA (10 μM) in the presence of DMC (0-10 μM) and then in the presence of AP (0-10 μM). λex = 280 nm.

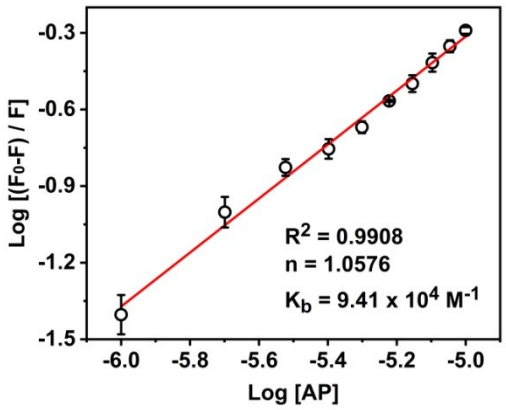

Fig. S11 The dependence of fluorescent signal [(F_0-F/F)] on concentrations of AP. Error bars = ± SD, n = 3. λ_{ex} = 280 nm.

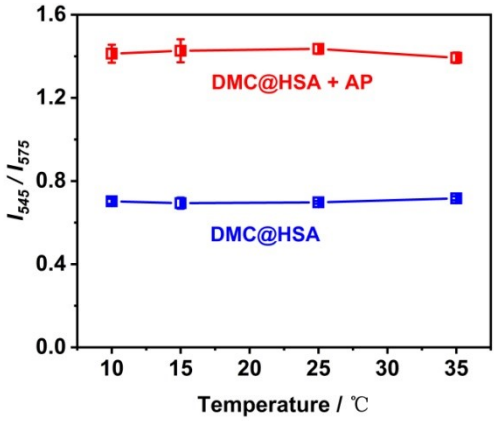

Fig. S12 The intensity ratio of DMC (10 μM) in the presence and absence of AP (100 μM) in different temperature conditions. λ_{ex} = 430 nm.

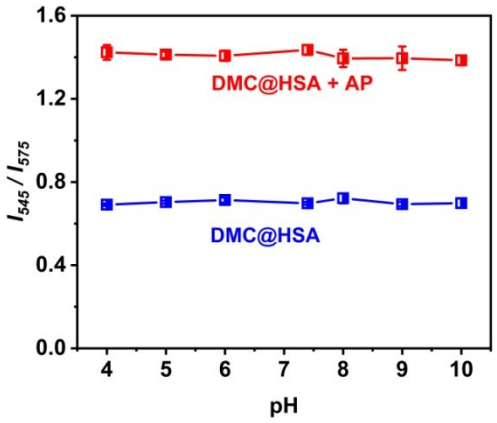

Fig. S13 The intensity ratio of DMC (10 μM) in the presence and absence of AP (100 μM) in different pH conditions. λ_{ex} = 430 nm.

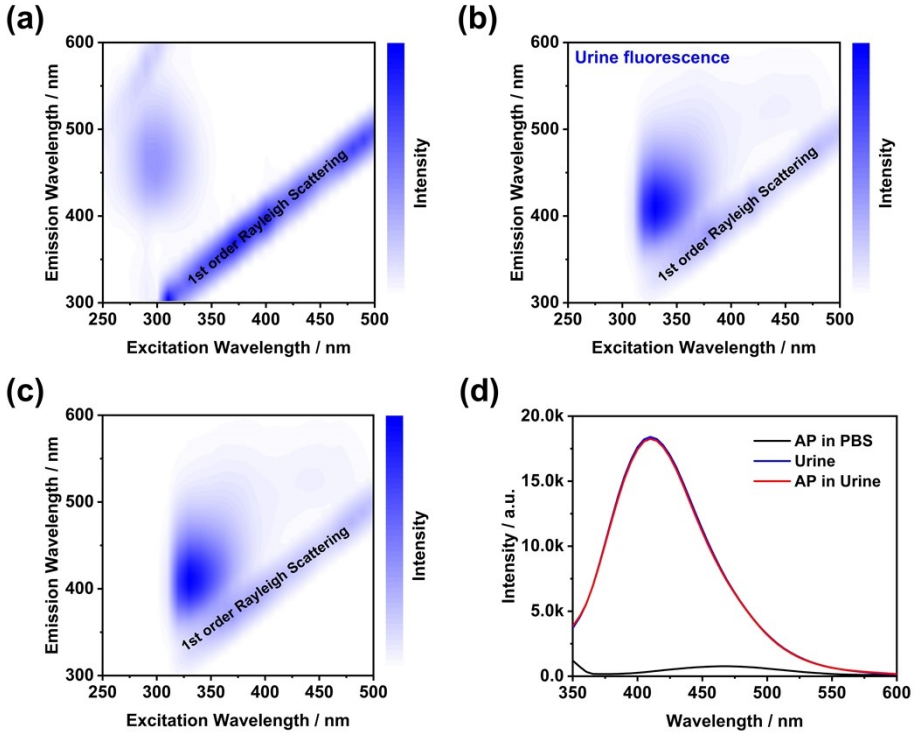

Fig. S14 Excitation-emission matrix fluorescence (EEMF) spectra of (a) AP in PBS (1 mM, pH ~ 7.4), (b) urine and (c) AP in urine. (d) The fluorescence spectra of AP in PBS (1 mM, pH ~ 7.4), urine and AP in urine. λ_{ex} = 330 nm

Table S1 Analytical techniques and performance of the developed methods for AP

No.	Technique	Response Time	LDR	LOD	Applications	Ref.
1	Electrochemical	/ [a]	0.01-10 μg/mL	10 ng/mL	Human plasma	2
2	HPLC-MS	1.0 min	1.0-200 ng/mL	1.0 ng/mL	Rat plasma	3
3	LC-MS	< 10 min	5.0-500 μg/L	2.0 μg/L	Human plasma	4
4	LC–MS/MS	6.6 min	1.0-300 ng/mL	1.0 ng/mL	Human plasma	5
5	UPLC-MS/MS	4.0 min	1.0-300 ng/mL	2.5 ng/mL	Human	6

					plasma	
6	RP-HPLC	15 min	1.0-3.0 μg/mL	0.3 μg/mL	/ [a]	[7]
7	HPLC-DAD	4.5 min	0.02-5.3 μg/mL	0.017 μg/mL	Human plasma	[8]
8	Chromogenic	/ [a]	70-2937 ng/mL	70 ng/mL	Human urine	[9]
9	UV-Vis spectrometric	/ [a]	5.0-25 μg/mL	0.23 μg/mL	/ [a]	[10]
10	Fluorometer	/ [a]	0.2-6.0 μg/mL	0.017 μg/mL	/ [a]	[11]
11	Fluorometer	/ [a]	0.05-3.0 μg/mL	8.598 ng/mL	Human plasma	[12]
12	Fluorescence	5 sec	2.04-28 μg/mL	2.04 μg/mL	Human urine	This work

Note: *a*: No data presented; LDR: Linear dynamic range; LOD: Limit of detection; HPLC-MS: High performance liquid chromatography-Mass spectroscopy; LC-MS: Liquid chromatography-Mass spectrometry; LC-MS/MS: Liquid chromatography tandem mass spectrometry; UHPLC-MS/MS: Ultra-high performance liquid chromatography tandem mass spectrometry; RP-HPLC: Reversed phase high performance liquid chromatography: HPLC-DAD: High performance liquid chromatography method coupled to diode array detection.

Table S2 Recovery Analysis of AP in urine samples

Sample	Spiked (μM) [a]	Detected (μM) [b]	Recovery (%) [c]	RSD (%) [d]
Urine	0.00	/ [e]	/ [e]	/ [e]
	20.0	20.6	103	15.7
	40.0	46.8	117	10.4
	60.0	55.4	92.3	6.87

Note: *a*: Represent the spiked concentration of AP; *b*: Represent the spiked concentration of AP; *c*: Were calculated by b/a; *d*: Relative standard deviation of three parallel experiments; *e*: Not detected.

3. References

1 S. Hadidi, *J. Biomol. Struct. Dyn.*, 2023, **41**, 7616–7626.

2 P. Shahbazi-Derakhshi, M. Abbasi, A. Akbarzadeh, A. Mokhtarzadeh, H. Hosseinpour and J. Soleymani, *RSC Adv.*, 2023, **13**, 21432–21440.

3 A. Jaber, I. Al-Ani, M. Hailat, E. Daoud, A. Abu-Rumman, Z. Zakaraya, B. J. M. Majeed, O. Al Meanazel and W. A. Dayyih, *Heliyon*, 2022, **08**, 11015.

4 X. Delavenne, P. Mismetti and T. Basset, *J. Pharm. Biomed. Anal.*, 2013, **78**–**79**, 150–153.

5 S. Baldelli, D. Cattaneo, P. Pignatelli, V. Perrone, D. Pastori, S. Radice, F. Violi and E. Clementi, *Bioanalysis*, 2016, **8**, 275–283.

6 K. I. Foerster, A. Huppertz, A. D. Meid, O. J. Müller, T. Rizos, L. Tilemann, W. E. Haefeli and J. Burhenne, *Anal. Chem.*, 2018, **90**, 9395–9402.

7 A. S. Chitale, P. Hamrapurkar, *Int. J. Adv. Res. Ideas Innov. Technol.* 2018, **04**, 367-370.

8 F. Gouveia, J. Bicker, J. Santos, M. Rocha, G. Alves, A. Falcão and A. Fortuna, *J. Pharm. Biomed. Anal.*, 2020, **181**, 113109.

9 J. Harenberg, S. Du, M. Wehling, S. Zolfaghari, C. Weiss, R. Krämer and J. Walenga, *Clin. Chem. Lab. Med.*, 2016, **54**, 275–283.

10 A. G. Radhika, A. Singh, A. Sowmya, A. Haque, V. Bakshi, N. Boggula, *Int. J. Pharm. Biol. Sci*., 2018, **08**, 1002-1008.

11 R. I. El-Bagary, E. F. Elkady, N. A. Farid and N. F. Youssef, *Spectrochim Acta A.*, 2017, **174**, 326–330.

12 A. S. Batubara, A. H. Abdelazim, M. Gamal, A. A. Almrasy and S. Ramzy, *Spectrochim Acta A.*, 2023, **290**, 122265.